Available online at www.sciencedirect.com
ScienceDirect
Trans. Nonferrous Met. Soc. China 32(2022) 3077−3087
Transactions of Nonferrous Metals Society of China
www.tnmsc.cn

Enhanced conversion mechanism of Al-goethite in gibbsitic bauxite under reductive Bayer digestion process

Guo-tao ZHOU, Yi-lin WANG, Tian-gui QI, Qiu-sheng ZHOU, Gui-hua LIU, Zhi-hong PENG, Xiao-bin LI

School of Metallurgy and Environment, Central South University, Changsha 410083, China

Received 9 August 2021; accepted 31 December 2021

Abstract: The conversion mechanism of Al-goethite under the action of different additives (lime or reductant for typical or reductive Bayer digestion) was investigated by thermodynamic calculation, XRD, and SEM−EDS. The results show that the formation of Fe-substituted hydrocalumite is crucial to converting Al-goethite to hematite during Bayer digestion by adding lime. However, the conversion proceeds more easily under the action of reductant due to the rapid formation of magnetite. Additionally, Bayer liquor composition significantly affects the product composition and also the conversion rate of Al-goethite. Compared to typical Bayer digestion with Al-goethite containing gibbsitic bauxite as raw material, the red mud yield of reductive Bayer digestion decreases from 39.02% to 31.19%, and the grade of TFe in red mud increases from 41.66% to 53.80%.

Key words: Al-goethite; conversion mechanism; Fe-substituted hydrocalumite; magnetite; Bayer process

1 Introduction

Alumina production worldwide reached 133 Mt in 2020 [1]. Nearly half of them are produced using gibbsitic bauxite from Guinea, Australia, and Indonesia. The prevalence of a certain amount of Al-substituted goethite (Al-goethite) in these bauxites is the main reason for the loss of alumina during the Bayer digestion process and the low beneficiation efficiency of iron minerals in red mud [2]. Also, the settling- separation performance of red mud slurry would be deteriorated due to the remainder goethite and the reversed boehmite [3−5]. Therefore, the rapid conversion of Al-goethite is of great importance for the optimization of the Bayer process and the comprehensive utilization of gibbsitic bauxite.

The phase conversion of Al-goethite in the pyrometallurgical process has been extensively investigated and numerous processes such as heating [6,7], mechanical grinding [8], and reductive roasting [9−13] have been proposed. However, these processes faced the problems of high energy consumption and huge equipment investment. Currently, more than 95% of alumina is produced by using the Bayer process, therefore, the hydrothermal conversion process which can incorporate into the current Bayer system has attracted much attention. Specifically, increasing the temperature, the concentration of caustic soda (especially in Bayer liquor composition, e.g., the concentration of caustic alkali and alumina) and adding hematite seed [14−17] are all beneficial to the conversion. In addition to the above measures, the use of additives is a common strategy, which consists of the following two main categories.

(1) Adding lime or other calcium-containing compounds. Studies [18,19] have shown that adding lime can promote the conversion of Al-goethite, but the mechanism is still unclear. One view [20] is that $Ca(OH)_2$ reacts with Al-goethite

---

Corresponding author: Yi-lin WANG, Tel/Fax: +86-731-88830453, E-mail: wang.yi.lin@outlook.com;
Xiao-bin LI, Tel/Fax: +86-731-88830453, E-mail: x.b.li@csu.edu.cn

DOI: 10.1016/S1003-6326(22)66004-7

at high temperatures to form the unstable intermediate compound $3CaO\cdot Fe_2O_3\cdot 2H_2O$, which further gradually dissociates into Fe_2O_3 and $Ca(OH)_2$. Another view [21] is that the conversion of Al-goethite is blocked by the formation of sodium titanate ($Na_2O\cdot 3TiO_2$) wrapped around the surface of Al-goethite during the Bayer digestion process, and the addition of lime effectively eliminates this blocking effect by converting sodium titanate to the more crystalline calcium titanate.

(2) Add reducing agents such as sugar, glycerol, and ferrous sulfate. LI [22] reports that the addition of 2% lime and 20 g/L glucose during the high-temperature digestion of Jamaican bauxite can achieve the conversion of iron minerals, resulting in coarse-grained red mud with a small specific surface area and improved settling and separation properties. LI et al [23] investigated the reaction behavior of Al-goethite in a high-iron gibbsitic bauxite from the Guangxi region in China and found that adding a reducing agent at 236 °C can promote the conversion of Al-goethite. PASECHNIK et al [24] proposed a method of hydrothermal digestion for handling red mud with the addition of $FeSO_4$ and lime, in which both the digestion of diaspore in the red mud and the conversion of hematite to magnetite can be implemented simultaneously. A recent study [25] has further demonstrated that accelerating this conversion facilitates the enrichment and beneficiation of iron minerals in the red mud. However, it should be noted that the above-mentioned studies do not provide a good explanation of the microscopic mechanism of Al-goethite conversion in the typical or reductive Bayer digestion process.

In this work, the mechanism of lime/reductant promotion of Al-goethite conversion was firstly analyzed based on thermodynamic calculations. Then, X-ray diffraction (XRD), scanning electron microscope (SEM), and energy dispersive spectrometer (EDS) were adopted to investigate the microscopic mechanism of the Al-goethite conversion. Finally, the validation was conducted in the Bayer digestion of gibbsitic bauxite.

2 Thermodynamic analysis

When the substitution ratio x of Al in Al-goethite [$Fe_{1-x}Al_xO\cdot OH$] was in the range of 0−0.33 (molar fraction), the thermodynamic calculation was carried out by setting x to be 0, 0.05, 0.20, and 0.33, respectively [26]. To clarify the degree of difficulty in the conversion of Al-goethite with different amounts of Al substitution, possible reactions of Al-goethite with reductant (hydrazine hydrate used in this case) during reductive Bayer digestion were speculated according to the reports in Ref. [27]. Besides, the reaction products of $CaO\cdot Al_2O_3\cdot Fe_2O_3$ in Bayer liquor [28,29] were expressed as $3CaO\cdot(Fe_2O_3)_x\cdot(Al_2O_3)_{1-x}\cdot 6H_2O$ ($C_3F_xA_{1-x}H_6$), and their thermodynamic data can be obtained using a Gibbs free energy estimation method [30]. Possible reactions of Al-goethite with lime or hydrazine hydrate in Bayer digestion are listed in Table 1, and the corresponding calculated Gibbs free energy changes ranging from 373 to 573 K were plotted in Fig. 1.

Table 1 Possible reactions of Al-goethite with lime or hydrazine hydrate in Bayer digestion

Reaction	Substitution ratio	No.
$Fe_{(1-x)}Al_xO\cdot OH+xOH^-=$ $(1-x)/2Fe_2O_3+(1-3x)/2H_2O+$ $xAl(OH)_4^-$	x=0	(1)
	x=0.05	(2)
	x=0.2	(3)
	x=0.33	(4)
$FeO\cdot OH+Al(OH)_4^-+3CaO+4H_2O=$ $3CaO\cdot(Fe_2O_3)_{0.5}\cdot(Al_2O_3)_{0.5}\cdot 6H_2O+OH^-$		(5)
$FeO\cdot OH+1/12N_2H_4\cdot H_2O=$ $1/3Fe_3O_4+1/12N_2+3/4H_2O$		(6)

From Fig. 1, the Δ_rG_m values for Reactions (1)−(4) were negative in the temperature range from 373 to 573 K, indicating that the reaction of $Fe_{1-x}Al_xO\cdot OH$ (x=0, 0.05, 0.20, 0.33) dehydrated to form Fe_2O_3 could spontaneously occur in Bayer liquor at above 373 K. However, even at 573 K, the Gibbs free energy changes for Reactions (1)−(4) are only −5.30, −2.51, −2.22, and −1.71 kJ/mol, respectively. This finding is consistent with the fact that goethite and Al-goethite are difficult to transform during the Bayer digestion process. In addition, the conversion of Al-goethite becomes more difficult due to increasing Al substitution, which is also consistent with previously reported results [31]. The Gibbs free energy change for Reaction (5) demonstrates that $C_3F_{0.5}A_{0.5}H_6$ could be formed thermo-dynamically in Bayer liquor with

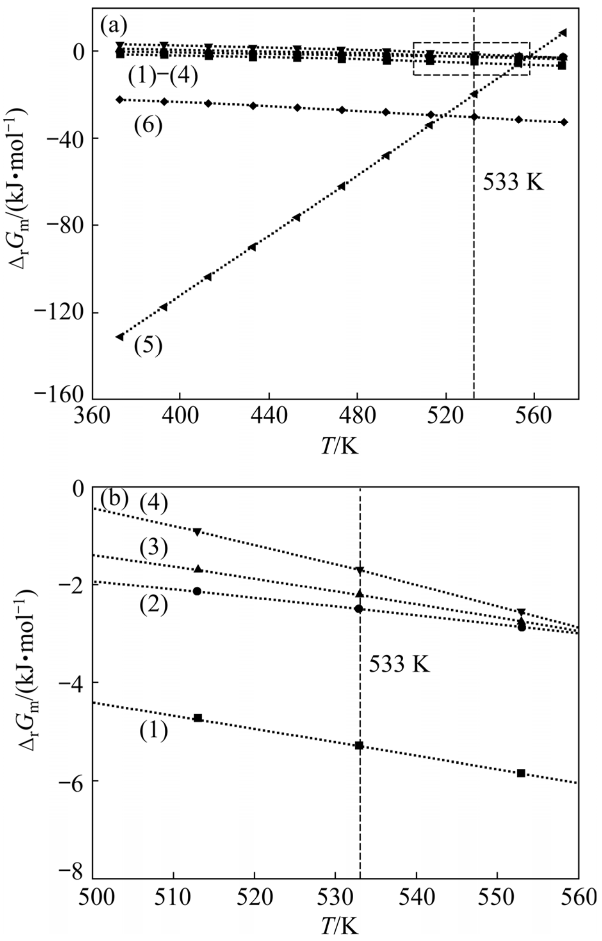

Fig. 1 Relationships between Δ_rG_m and temperature for reactions in Table 1: (a) Reactions (1)−(6); (b) Enlarged map of rectangle in (a)

lime. This phenomenon implies that the reason for facilitating the conversion of goethite may be due to the formation of the corresponding Fe−Al−Ca compounds. The Gibbs free energy change of Reaction (5) increases with increasing temperature. This reason may be due to the easy decomposition of $C_3F_{0.5}A_{0.5}H_6$, which is consistent with literature report [20]. In the presence of reductant (hydrazine hydrate), goethite can be transformed directly into magnetite according to Reaction (6) and the trend of this reaction becomes more obvious with the increasing temperature. The comparison between Reactions (5) and (6) indicates that the amounts of lime and hydrazine hydrate required to transform 1 g of goethite were 1.888 and 0.047 g, respectively. The smaller amount of hydrazine hydrate required to achieve complete conversion of the goethite compared to the lime additive, meaning that reductive digestion may be more advantageous.

3 Experimental

3.1 Materials

The preparation methods of Al-goethite were based on previous report [32]. Briefly, about 5 and 0.5 mol/L KOH solutions were successively added to the mixture of $Fe(NO_3)_3·9H_2O$ and $Al(NO_3)_3·9H_2O$ solutions at a rate of 20 mL/min to adjust the pH at 12.8±0.1. The suspensions were stirred for 60 min and aged at 70 °C for 14 d. The final product was washed with deionized water, dried in an oven at 50 °C, and stored in polypropylene containers in a desiccator. The XRD pattern and SEM image of the synthetic Al-goethite particles are shown in Fig. 2. The characteristic peaks of the Al-goethite samples match well with the standard card of goethite (ICSD No. 29-0713), revealing that no other Fe-bearing phase exists. The high peak intensities indicate good crystallinity of the samples. The SEM image of pure Al-goethite shows typical acicular and rod-like morphology, and the length and width are approximately 1 and 0.2 μm, respectively, indicating the presence of only one phase, which is highly consistent with the powder XRD results. The chemical composition

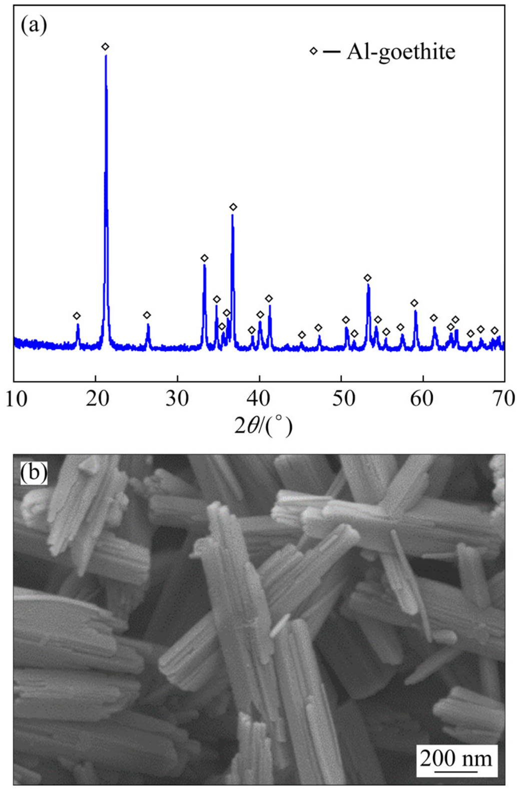

Fig. 2 XRD pattern (a) and SEM image (b) of synthetic Al-goethite

analysis by using an inductively coupled plasma emission spectrometer (ICP-OES) shows that the main content is iron oxide (85.84 wt.% Fe_2O_3) followed by aluminum oxide (3.05 wt.% Al_2O_3), thus forming Al-goethite.

The bauxite used in the experiments was a Guinea gibbsitic bauxite with a composition of 42.47 wt.% Al_2O_3, 24.34 wt.% Fe_2O_3, and 2.32 wt.% SiO_2. The mineral compositions of gibbsitic bauxites were estimated via XRD and chemical analyses, and the semi-quantitative results are listed in Table 2. Al-goethite and boehmite account for 16.9 wt.% and 2.3 wt.% in gibbsitic bauxite, respectively. Therefore, high-temperature Bayer digestion should be adopted to improve the alumina recovery. The Bayer liquor was prepared by dissolving $Al(OH)_3$ and NaOH. Lime (CaO) was obtained by roasting $CaCO_3$ in the muffle furnace at 950 °C for 120 min. $Fe(NO_3)_3\cdot 9H_2O$, $Al(NO_3)_3\cdot 9H_2O$, KOH, NaOH, $CaCO_3$, and $Al(OH)_3$ were of analytical grade (>99%) and purchased from Shanghai Macklin Biochemical Co., Ltd., China.

Table 2 Estimated mineral compositions of gibbsitic bauxite (wt.%)

Gibbsite	Boehmite	Hematite	Al-goethite
59.6	2.3	10.8	16.9
Kaolinite	Quartz	Anatase	Rutile
1.3	1.8	1.5	1.2

3.2 Methods

Simulated digestion experiments were carried out in the molten mixed nitrate salt cells (YYL−150ML/6, Dingda Chemical Machinery Co., Ltd., China). Starting materials, namely, 1 g Al-goethite samples (or 23.6 g gibbsitic bauxite) and additives (lime or hydrazine hydrate), reacted with 100 mL Bayer liquor in a 150 mL sealed rotating steel reactor immersed in molten-mixed nitrate salt cell at a preset temperature of 533 K. In the process of digesting gibbsitic bauxite, 2×*d*15 mm and 2×*d*4 mm steel balls were added into the reactor in advance to enhance stirring. After the reaction, the reactors were taken out of the cell and immediately cooled with tap water. Subsequently, the obtained slurry was filtered, and the filter cake was washed with hot water and dried at 100 °C for 6 h before analysis. The $N_2H_4\cdot H_2O$ was of analytical grade (>98%) and purchased from Shanghai Aladdin Biochemical Technology Co., Ltd., China.

3.3 Characterization

The mineral phases were characterized by an X-ray diffractometer (Empyrean2, PANalytical, Netherlands) using Cu K_α radiation at a scan rate of 5 (°)/min. Microscopic surface morphology and microscale composition analysis were conducted with a field emission scanning electron microscope (MIRA3-LMH, TESCAN, Czech Republic) and an energy dispersive spectrometer (EDX-MAX20, Oxford, England). Chemical analysis of samples was performed via the fusion method (750 °C for 15 min with a mixture of NaOH followed by direct dissolution in boiling deionized water) with an inductive coupled plasma emission spectrometer (ICAP7400 Radial, Thermo Fisher Scientific, USA).

The proportion of converted Al-goethite relative to the total iron oxides was employed to present the extent of the goethite conversion [33]. The goethite (110) peak from the XRD patterns along with the hematite (110) and magnetite (311) peaks was used to calculate the recovery rate of Al-goethite (η(AG)) (Eq. (7)). The intensities were calculated from areas under the peaks.

$$\eta(\mathrm{AG})=1-\frac{I_{(\mathrm{goethite},110)}}{I_{(\mathrm{goethite},110)}+I_{(\mathrm{hematite},110)}+I_{(\mathrm{magnetite},311)}} \quad (7)$$

where I was the intensity of the corresponding goethite, hematite, and magnetite peak at crystal planes (110), (110), and (311), respectively.

The alumina recovery during Bayer digestion was calculated with Eq. (8):

$$\eta(\mathrm{Al_2O_3})=\frac{(\mathrm{A/S})_1-(\mathrm{A/S})_2}{(\mathrm{A/S})_1-1} \quad (8)$$

where $\eta(Al_2O_3)$ is the recovery of alumina, and $(A/S)_1$ and $(A/S)_2$ are the mass ratios of alumina to silica in gibbsitic bauxite and red mud, respectively.

4 Results and discussion

4.1 Conversion of Al-goethite by adding lime

Thermodynamic analysis results reveal that Al-goethite can react with lime to form $C_3F_{0.5}A_{0.5}H_6$ in the Bayer liquor, which may have an impact on the conversion of Al-goethite to hematite. To clarify the promotion mechanism, the interaction behavior of lime (0.2 g) and Al-goethite (1 g) was studied separately at 260 °C for 40 min under various compositions of the Bayer liquor (the concentration of Na_2O_K (caustic alkali in Na_2O) remained consistent at 170 g/L, and those of Al_2O_3 were 90 and 193 g/L, corresponding to α_k (the ratio of the concentration of Na_2O_K to that of Al_2O_3) being 3.12 and 1.45, respectively. The XRD patterns of Al-goethite conversion products and the η(AG) calculated according to Eq. (7) are shown in Fig. 3 and Table 3, respectively. Combined with the blank experimental results in Fig. 3 and Table 3, it can be found that the spontaneous conversion process of synthetic Al-goethite in Bayer liquor is relatively slow. The conversion rate of Al-goethite is less than 20% in either α_k=1.45 or α_k=3.12 Bayer liquor under high-temperature Bayer digestion conditions. Increasing the α_k of Bayer liquor favors the conversion, but the efficiency is very limited, with η(AG) only ranging from 9.45% to 14.78%, indicating that α_k is not a key factor that influences the conversion of Al-goethite under these conditions. The reason is that synthetic Al-goethite is stable and difficult to convert in the absence of additives. In contrast, the promotion of Al-goethite conversion by adding lime and increasing the α_k can be seen in the control group results with the conversion rate of Al-goethite increasing from 9.45% and 14.78% to 39.63% and 100%, respectively. From the diffraction patterns of the corresponding products, the hydrocalumites formed by lime reaction in Bayer liquors with different α_k differ significantly, as $4CaO\cdot 3Al_2O_3\cdot 3H_2O$ and $3CaO\cdot Al_2O_3\cdot 6H_2O$, respectively. Therefore, the effect of lime on upgrading the conversion of Al-goethite may be related to the presence of calcium and aluminum compounds with different morphologies.

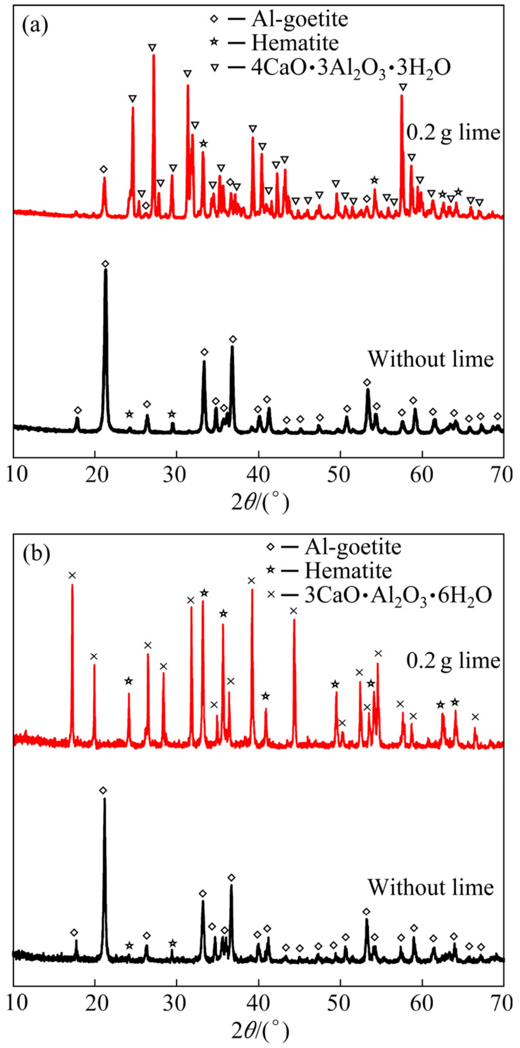

Fig. 3 XRD patterns of reaction products of Al-goethite and lime in Bayer liquors with different α_k (1 g Al-goethite, 0.2 g lime, T=260 °C, t=40 min, 100 mL Bayer liquid, and 170 g/L Na_2O_K): (a) α_k=1.45; (b) α_k=3.12

Table 3 Influence of α_k and lime dosage on conversion rate of Al-goethite to hematite (1 g Al-goethite, 260 °C, 40 min, 100 mL Bayer liquid, and 170 g/L Na_2O_K)

No.	α_k	Lime dosage/g	η(AG)/%
1	1.45	0	9.45
2	1.45	0.2	39.63
3	3.12	0	14.78
4	3.12	0.2	100

It should be noted that the expected interaction products of Al-goethite and lime were not observed in the XRD patterns (Fig. 3). Hence, the SEM and EDS analyses of the reaction products formed in Bayer liquors with different α_k were performed, and the results are shown in Fig. 4. From Fig. 4, the products contain mainly unconverted rod-shaped Al-goethite and cubic hydrocalumite. The EDS data further indicate that the Ca/Al molar ratios are 1.24 and 1.99, respectively, both higher than the 0.67 and 1.50 determined by diffraction results in Fig. 3. The results indicate that the surface Al atoms should be replaced by the detected Fe atoms to form the Fe-substituted $4CaO\cdot x Fe_2O_3\cdot (3-x)Al_2O_3\cdot 3H_2O$ or $3CaO\cdot x Fe_2O_3\cdot (1-x)Al_2O_3\cdot 6H_2O$ hydrocalumites. In addition, it can be inferred from good cubic morphology of the Fe-substituted hydrocalumite

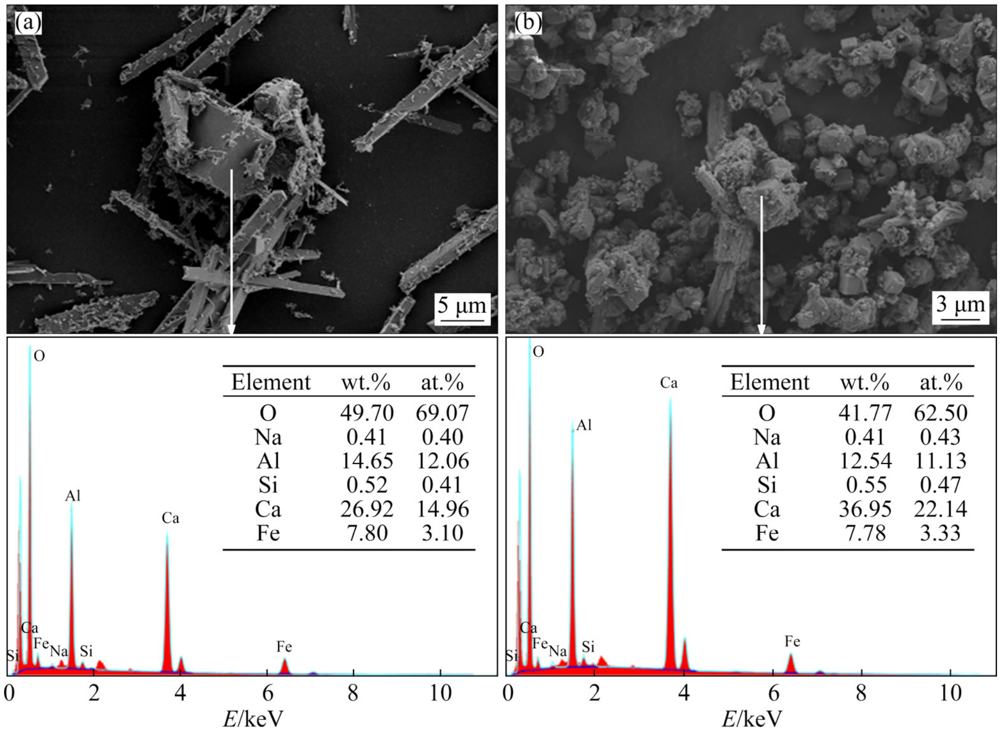

(a)

Element	wt.%	at.%
O	49.70	69.07
Na	0.41	0.40
Al	14.65	12.06
Si	0.52	0.41
Ca	26.92	14.96
Fe	7.80	3.10

(b)

Element	wt.%	at.%
O	41.77	62.50
Na	0.41	0.43
Al	12.54	11.13
Si	0.55	0.47
Ca	36.95	22.14
Fe	7.78	3.33

Fig. 4 SEM images and and EDS spectra of reaction products of Al-goethite and lime in Bayer liquor with different α_k (1 g Al-goethite, 0.2 g lime, 260 °C, 40 min, 100 mL Bayer liquid, and 170 g/L Na_2O_K): (a) α_k=1.45; (b) α_k=3.12

products that the embedding of iron ions occurs during the hydrocalumite crystallization. Meanwhile, it is further suggested that the hydrocalumite forms faster instead under the condition of low α_k, resulting in the inability to embed more iron ions simultaneously, which is the main reason for the weak lime promotion under this condition.

In summary, it can be concluded that calcium-containing additives can promote the conversion of Al-goethite to hematite from the substitution of Fe and Al elements occurring during the formation of Fe-substituted hydrocalumite, rather than the direct formation of iron−calcium compounds.

4.2 Conversion of Al-goethite by adding reductant

In previous studies [34−36], adding reductant (iron) in the reductive Bayer digestion was conducive to the conversion of hematite to magnetite, and the reaction was carried out from the outside to the inside of the iron mineral particles. To recover alumina from Al-goethite, structural reconstruction of Fe-bearing minerals is inevitably required, so the reaction process may differ significantly from that of hematite. To clarify the mechanism of this process, the behavior of the reductant (hydrazine hydrate, 0.2 g) and Al-goethite (1 g) was examined under typical caustic ratio conditions of the digestion liquor at 260 °C. The XRD patterns of conversion products and η(AG) are shown in Fig. 5 and Table 4, respectively.

From Fig. 5 and Table 4, under the action of reductant for 40 min, the Al-goethite is completely converted and the η(AG) has reached 100%. Comparing the data in Table 4, it can be found that the adding reducing agent has a much higher conversion promotion effect than adding lime, and the conversion efficiency improvement for Al-goethite in low α_k Bayer liquor is also considerable, implying that the difference in the action of reducing agent and lime should be related to the microscopic reaction mechanism of Al-goethite. From Fig. 5 and Table 4, it is known that η(AG) does not differ much under different α_k conditions (α_k=1.45 and α_k=3.12), but the product composition varies significantly.

At 40 min of reaction, the conversion product in the low α_k Bayer liquor was dominated by hematite, while in the high α_k Bayer liquor it corresponded to magnetite. Meanwhile, only characteristic peak of magnetite appears in the

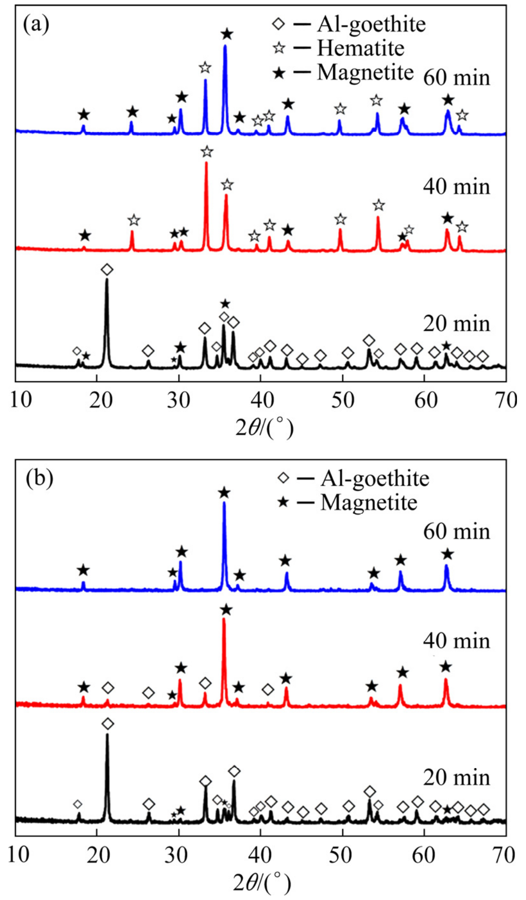

Fig. 5 XRD patterns of reaction products of Al-goethite and hydrazine hydrate in Bayer liquor for 20, 40, and 60 min (1 g Al-goethite, 0.2 g hydrazine hydrate, 260 °C, 100 mL Bayer liquid, and Na_2O_K 170 g/L): (a) α_k=1.45; (b) α_k=3.12

Table 4 Influence of α_k and time on conversion rate of Al-goethite to hematite and/or magnetite (1 g Al-goethite, 0.2 g hydrazine hydrate, 260 °C, 100 mL Bayer liquid, and 170 g/L Na_2O_K)

No.	α_k	Time/min	η(AG)/%
1	1.45	20	19.24
2	1.45	40	100
3	1.45	60	100
4	3.12	20	11.73
5	3.12	40	96.17
6	3.12	60	100

diffraction pattern of the product obtained in the low α_k Bayer liquor at 60 min. The results suggest that the conversion of Al-goethite to magnetite during the Bayer process evolved in two ways: (1) when the α_k is low, hematite as interphase can be firstly formed, and hematite is then converted to magnetite; (2) when the α_k is high, Al-goethite is directly and efficiently transformed to magnetite. It should be noted that the Fe ions in Al-goethite and hematite are Fe(III), but the reducing agent still significantly facilitates the conversion of Al-goethite to hematite, which is not well explained by the relationship between the α_k and the concentration of Fe(III) in Bayer liquor. Based on the obvious diffraction peaks of magnetite in the reaction product at 20 min, we believe that the reason for this process may come from the fact that the Al-goethite was firstly transformed to form part of the magnetite, which underwent structural reconstruction and formed more reactive sites, in turn leading to the rapid dissolution of Al-goethite and its massive crystallization and precipitation into hematite in the oxidizing atmosphere of the high-temperature aqueous solution system.

In order to further understand the Al-goethite conversion process, the SEM images of the reaction products following the treatment of Al-goethite and hydrazine hydrate mixture in Bayer liquor at 260 °C for different time are shown in Fig. 6. Consistent with the above analysis, the formation of microcrystalline minerals on the surface of Al-goethite was observed in SEM images of the initial conversion product (20 min) of low α_k Bayer liquor, which, combined with diffraction results, should be the initial formation of magnetite. As the reaction time increased to 40 min, hexagonal flaky hematite was observed as shown in Fig. 6(b). The hexagonal flaky hematite is further dissolved and resolved into magnetite as the reaction time continues to increase to 60 min, as demonstrated in Fig. 6(c). The SEM images of the reaction products from the treatment of Al-goethite and hydrazine hydrate mixture in Bayer liquor with α_k=3.12 at 260 °C for different time (Figs. 6(e−f)) also show that the hydrothermal conversion of Al-goethite to magnetite experiences Al-goethite dissolution, fine grain magnetite crystallization precipitation and growth.

Therefore, by studying the interactions between the reducing agent and Al-goethite, it can be concluded that the reducing agent can significantly promote the conversion of Al-goethite to hematite or magnetite. Moreover, the degree of promotion is better than that of lime additives.

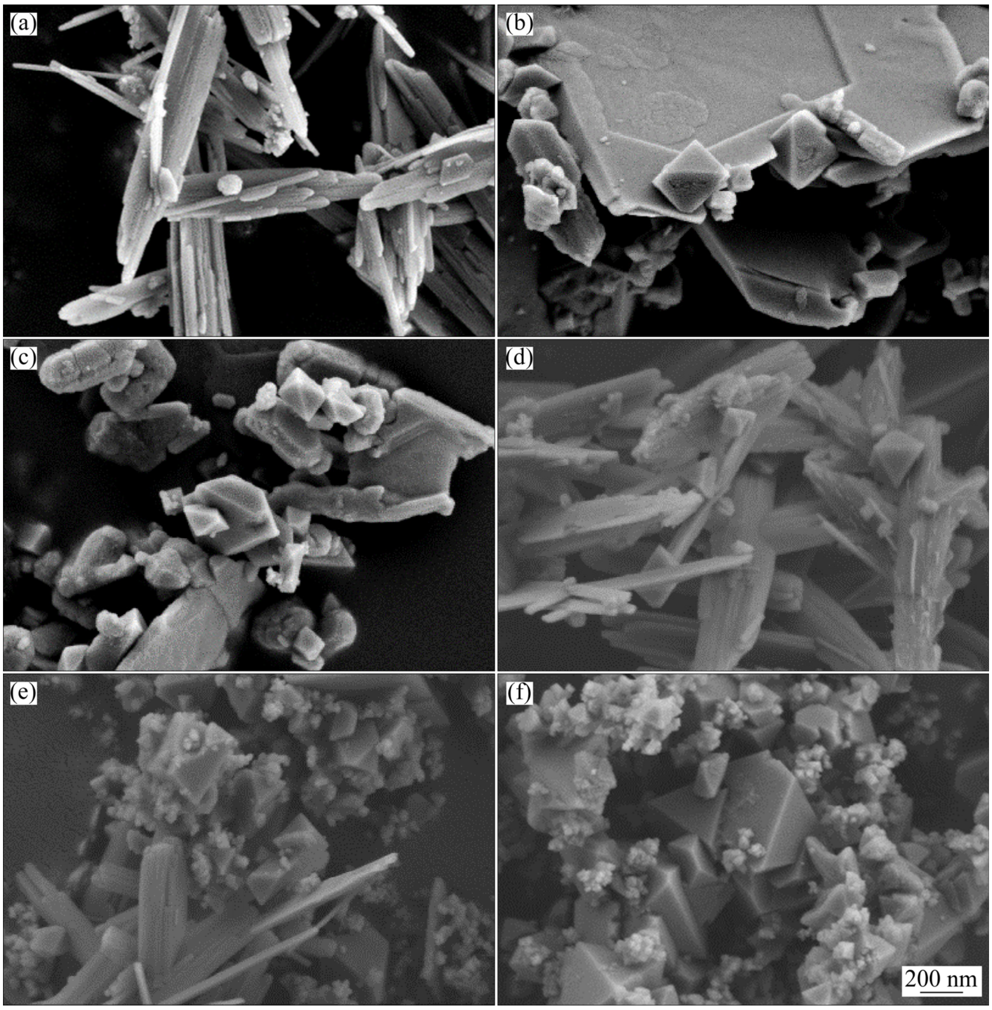

Fig. 6 SEM images of reaction products of Al-goethite and hydrazine hydrate in Bayer liquor with different α_k for different time (1 g Al-goethite, 0.2 g hydrazine hydrate, 260 °C, 100 mL Bayer liquid, and 170 g/L Na_2O_K): (a) α_k=1.45, 20 min; (b) α_k=1.45, 40 min; (c) α_k=1.45, 60 min; (d) α_k=3.12, 20 min; (e) α_k=3.12, 40 min; (f) α_k=3.12, 60 min

4.3 Conversion of Al-goethite in gibbsitic bauxite during Bayer digestion

The conversion mechanism of pure Al-goethite promoted by adding lime or hydrazine hydrate has been previously clarified. Therefore, digestion experiments of a high-iron gibbsitic bauxite were conducted using 23.6 g of bauxite and 100 mL of Bayer liquor (170 g/L Na_2O_K and α_k=3.12) at 260 °C for 60 min to further verify the above-mentioned results and elaborate the influence of goethite conversion on the form and enrichment degree of Fe minerals in the red mud. Either lime (4 wt.% of the bauxite) or hydrazine hydrate (0.9 wt.% of the bauxite) was added. Table 5 and Fig. 7 show the chemical and mineral component analyses of the resultant red mud.

In Table 5, the η(AG) and $\eta(Al_2O_3)$ in the typical Bayer digestion are only 30.59% and 91.50%, respectively, indicating that substantial Al-goethite is present in the red mud. This result is consistent with the previous analysis that the conversion of Al-goethite is difficult during Bayer digestion. However, the addition of lime or hydrazine hydrate can improve the conversion of goethite or Al-goethite to hematite in Bayer digestion. Under the action of 4.00% lime or 0.90% hydrazine hydrate, the conversion rate of Al-goethite is 100%. The XRD results in Fig. 7 further indicate that the red mud generated from reductive Bayer digestion is mainly composed of hematite rather than magnetite, which is consistent with the result that reductant greatly promotes the conversion of Al-goethite to hematite when the α_k is low.

Table 5 Experimental results of gibbsitic bauxite digested with various additives (23.6 g bauxite, 100 mL Bayer liquid, 170 g/L Na_2O_K, α_k=3.12, 260 °C, and 60 min)

Additive	Dosage/%	Red mud yield/%	Chemical composition/wt.%			η(AG)/%	$\eta(Al_2O_3)$/%
			Al_2O_3	SiO_2	TFe		
Null	−	36.28	10.35	4.19	46.98	30.59	91.50
Lime	4.00	39.02	6.27	4.44	41.66	100	97.61
Hydrazine hydrate	0.90	31.19	6.07	4.86	53.80	100	98.56

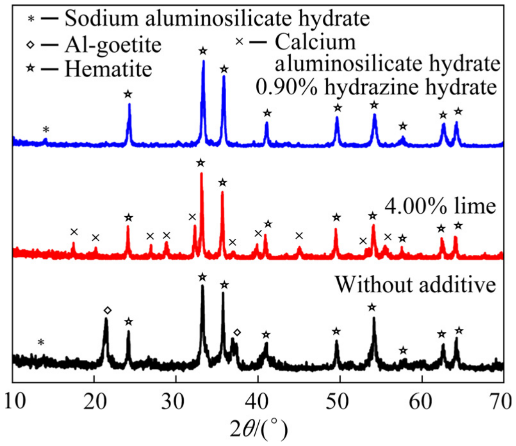

Fig. 7 XRD patterns of gibbsitic bauxite digested with various additives (23.6 g bauxite, 100 mL Bayer liquid, 170 g/L Na_2O_K, α_k=3.12, 260 °C, and 60 min)

The $\eta(Al_2O_3)$ values reached 97.61% and 98.56% with adding lime and hydrazine hydrate, respectively. However, the TFe grade in the red mud is only 41.66% due to the inevitable increase in the amount of red mud because of the Ca-bearing additives; whereas the TFe in the red mud with a reducing agent is as high as 53.80%, which can further synergize the disposal of the steel industry. Therefore, reductive Bayer digestion is more conducive to the resource utilization of red mud.

5 Conclusions

(1) Lime additives can promote the conversion of Al-goethite to hematite from the substitution of Fe and Al elements during the formation of Fe-substituted hydrocalumite, rather than directly forming iron and calcium compounds. The higher the α_k is, the higher the Fe substitution rate in the formed hydrocalumite is.

(2) The reducing agent can significantly promote the conversion of Al-goethite, which is better than lime additives. When the α_k is high, Al-goethite is directly converted to magnetite under the action of the reducing agent. When the α_k is low, hematite is firstly formed in large quantities.

(3) The addition of lime or a reducing agent can improve the hydrothermal conversion of Al-goethite in gibbsitic bauxite during Bayer digestion, which increases the digestion ratio of alumina. Meanwhile, the use of a liquor reducing agent can significantly reduce the production of red mud, thereby greatly increasing the iron concentrate grade of TFe in the red mud to 53.80%.

Acknowledgments

The authors gratefully appreciate the financial support provided by the National Natural Science Foundation of China (No. 52104353).

References

[1] NOVELL S. Statistics of alumina production [DB/OL]. 2021−06−09. https://international-aluminium.org/statistics/alumina-production.

[2] HIND A R, BHARGAVA S K, GROCOTT S C. The surface chemistry of Bayer process solids: A review [J]. Colloids and Surfaces A: Physicochemical and Engineering Aspects, 1999, 146(1/2/3): 359−374.

[3] POWELL K A, KIRWAN L J, HODNETT K, LAWSON D, RIJKEBOER A. Characterisation of alumina and soda losses associated with the processing of goethitic rich jamaican bauxite [C]//The 138th TMS Annual Meeting. San Francisco: TMS, 2009: 151−156.

[4] LAWSON D, RIJKEBOER A, DAJKOVICH D, JACKSON M, LAWRENCE H. Approaches to the processing of Jamaican bauxite with high goethite content [C]//The 143rd TMS Annual Meeting Exhibition. Switzerland: Springer, 2014: 11−18.

[5] WANG Meng, HU Hui-ping, LIU Jin-wei. Negative effects of dissolved organic compounds on settling performance of goethite in Bayer red mud [J]. Transactions of Nonferrous Metals Society of China, 2017, 27(2): 429−439.

[6] GIALANELLA S, GIRARDI F, ISCHIA G, LONARDELLI I, MATTARELLI M, MONTAGNA M. On the goethite to hematite phase transformation [J]. Journal of Thermal Analysis and Calorimetry, 2010, 102(3): 867−873.

[7] WOLSKA E, SZAJDA W, PISZORA P. Determination of solid solution limits based on the thermal behaviour of aluminium substituted iron hydroxides and oxides [J].

Journal of Thermal Analysis, 1992, 38(9): 2115−2122.

[8] LEMINE O M. Transformation of goethite to hematite nanocrystallines by high energy ball milling [J]. Advances in Materials Science and Engineering, 2014, 2014: 589146.

[9] WU Y, FANG M, LAN L D, ZHANG P, RAO K V, BAO Z Y. Rapid and direct magnetization of goethite ore roasted by biomass fuel [J]. Separation and Purification Technology, 2012, 94: 34−38.

[10] JANG K O, NUNNA V R M, HAPUGODA S, NGUYEN A V, BRUCKARD W J. Chemical and mineral transformation of a low grade goethite ore by dehydroxylation, reduction roasting and magnetic separation [J]. Minerals Engineering, 2014, 60: 14−22.

[11] NUNNA V, HAPUGODA S, POWNCEBY M I, SPARROW G J. Beneficiation of low-grade, goethite-rich iron ore using microwave-assisted magnetizing roasting [J]. Minerals Engineering, 2021, 166: 106826.

[12] RAVISANKAR V, VENUGOPAL R, BHAT H. Investigation on beneficiation of goethite-rich iron ores using reduction roasting followed by magnetic separation [J]. Mineral Processing and Extractive Metallurgy: Transactions of the Institutions of Mining and Metallurgy, 2019, 128(3): 175−182.

[13] ZHANG Y Y, GAO Q J, ZHAO J, LI M Y, QI Y H. Semi-smelting reduction and magnetic separation for the recovery of iron and alumina slag from iron rich bauxite [J]. Minerals, 2019, 9(4): 223.

[14] PAN Xiao-lin, YU Hai-yan，TU Gan-feng，BI Shi-wen. Effect of lime on digestion of gibbsitic bauxites at low temperature [J]. Journal of Northeastern University (Natural Science), 2013, 34(4): 551−555. (in Chinese)

[15] SOLYMAR K, SAJO I, STEINER J, ZOLDI J. Characteristics and separability of red mud [C]//The 21st TMS Annual Meeting. San Francisco: TMS, 1992: 209−223.

[16] SUSS A, FEDYAEV A, KUZNETZOVA N, DAMASKIN A, KUVYRKINA A, PANOV A, PAROMOVA I, LUKYANOV I. Technology liquors to increase alumina recovery from aluminogoethitic bauxites [C]//The 139th TMS Annual Meeting. Switzerland: Minerals, Metals and Materials Soc, 2010: 53−56.

[17] MURRAY J, KIRWAN L, LOAN M, HODNETT B K. In-situ synchrotron diffraction study of the hydrothermal transformation of goethite to hematite in sodium aluminate solutions [J]. Hydrometallurgy, 2009, 95(3/4): 239−246.

[18] PAN Xiao-lin, YU Hai-yan, DONG Kai-wei, TU Gan-feng, BI Shi-wen. Pre-desilication and digestion of gibbsitic bauxite with lime in sodium aluminate liquor [J]. International Journal of Minerals, Metallurgy, and Materials, 2012, 19(11): 973−977.

[19] SMITH P. Reactions of lime under high temperature Bayer digestion conditions [J]. Hydrometallurgy, 2017, 170: 16−23.

[20] WHITTINGTON B I. The chemistry of CaO and $Ca(OH)_2$ relating to the Bayer process [J]. Hydrometallurgy 1996, 43(1/2/3): 13−35.

[21] XU Bin-gan, SMITH P, WINGATE C, DE SILVA L. The effect of calcium and temperature on the transformation of sodalite to cancrinite in Bayer digestion [J]. Hydrometallurgy, 2010, 105(1/2): 75−81.

[22] LI L Y. A study of iron mineral transformation to reduce red mud tailings [J]. Waste Management, 2001, 21(6): 525−534.

[23] LI Xiao-bin, KONG Lian-lian, QI Tian-gui, ZHOU Qiu-sheng, PENG Zhi-hong, LIU Gui-hua. Effect of alumogoethite in Bayer digestion process of high-iron gibbsitic bauxite [J]. The Chinese Journal of Nonferrous Metals, 2013, 23(2): 543−548. (in Chinese)

[24] PASECHNIK L A, SKACHKOV V M, BOGDANOVA E A, CHUFAROV A Y, KELLERMAN D G, MEDYANKINA I S, YATSENKO S P. A promising process for transformation of hematite to magnetite with simultaneous dissolution of alumina from red mud in alkaline medium [J]. Hydrometallurgy, 2020, 196: 105438.

[25] LI Xiao-bin, ZHOU Zhao-yu, WANG Yi-lin, ZHOU Qiu-sheng, QI Tian-gui, LIU Gui-hua, PENG Zhi-hong. Enrichment and separation of iron minerals in gibbsitic bauxite residue based on reductive Bayer digestion [J]. Transactions of Nonferrous Metals Society of China, 2020, 30(7): 1980−1990.

[26] SCHEINOST A C, SCHULZE D G, SCHWERTMANN U. Diffuse reflectance spectra of Al substituted goethite: A ligand field approach [J]. Clays and Clay Minerals, 1999, 47(2): 156−164.

[27] SOBHANI A, SALAVATI-NIASARI M. Synthesis and characterization of a nickel selenide series via a hydrothermal process [J]. Superlattices and Microstructures, 2014, 65: 79−90.

[28] MAL'TS N S, KORNEEV V I, SUSS A G, SENNIKOV S G, FIRFAROVA I B. Effect of the leaching conditions on the extraction of alumina from aluminogoethites [J]. Tsvetnye Metally, 1983, 10: 45−47.

[29] MAL′TS N S, PODDYMOV V P, RUDASHEVSKII L S, KISELEV V E. Mechanism of the intensifying action of lime on bauxite leaching kinetics [J]. Tsvetnye Metally, 1985, 11: 40−43.

[30] LI Xiao-bin, YANG Li-qun, ZHOU Qiu-sheng, QI Tian-gui, LIU Gui-hua, PENG Zhi-hong. A split-combination method for estimating the thermodynamic properties (Go and Ho) of multicomponent minerals [J]. Applied Clay Science, 2020, 185: 105406.

[31] RUAN H D, FROST R L, KLOPROGGE J T, DUONG L. Infrared spectroscopy of goethite dehydroxylation: III. FT-IR microscopy of in situ study of the thermal transformation of goethite to hematite [J]. Spectrochimica Acta (Part A): Molecular and Biomolecular Spectroscopy, 2002, 58(5): 967−981.

[32] HIEMSTRA T, VAN RIEMSDIJK W H, BOLT G H. Multisite proton adsorption modeling at the solid/solution interface of (hydr)oxides: A new approach: II. Application to various important (hydr)oxides [J]. Journal of Colloid and Interface Science, 1989, 133(1): 105−117.

[33] WU Fei. Aluminous goethite in the Bayer process and its impact on alumina recovery and settling [D]. Perth: Curtin University, 2012: 152−154.

[34] WANG Yin-lin, LI Xiao-bin, ZHOU Qiu-sheng, QI Tian-gui, LIU, Gui-hua, PENG Zhi-hong, ZHOU Ke-chao. Effects of Si-bearing minerals on the conversion of hematite into magnetite during reductive Bayer digestion [J].

Hydrometallurgy, 2019, 189: 105126.

[35] LI Xiao-bin, WANG Yi-lin, ZHOU Qiu-sheng, QI Tian-gui, LIU Gui-hua, PENG Zhi-hong, WANG Hong-yang. Transformation of hematite in diasporic bauxite during reductive Bayer digestion and recovery of iron [J]. Transactions of Nonferrous Metals Society of China, 2017, 27(12): 2715−2726.

[36] LI Xiao-bin, LIU Nan, QI Tian-gui, WANG Yi-lin, ZHOU Qiu-sheng, PENG Zhi-hong, LIU Gui-hua. Conversion of ferric oxide to magnetite by hydrothermal reduction in Bayer digestion process [J]. Transactions of Nonferrous Metals Society of China, 2015, 25(10): 3467−3474.

还原拜尔法溶出三水铝石矿中铝针铁矿的强化转化机理

周国涛，王一霖，齐天贵，周秋生，刘桂华，彭志宏，李小斌

中南大学 冶金与环境学院，长沙 410083

摘　要：通过热力学计算、XRD 与 SEM−EDS 研究不同添加剂(石灰/还原剂分别对应典型/还原拜耳法溶出)作用下铝针铁矿的转化机理。结果表明，形成含铁水铝钙石相是石灰促进这一转化的主要机制；而在还原剂作用下，由于磁铁矿的生成，铝针铁矿的转化更易发生。此外，拜耳溶液成分显著影响针铁矿转化过程产物组成和转化速率。与以含铝针铁矿的三水铝石为原料的典型拜耳法溶出相比，还原拜耳溶出赤泥的产出率由 39.02%降低至 31.19%，总铁含量(TFe)由 41.66%提高至 53.80%。

关键词：铝针铁矿；转化机制；含铁水铝钙石；磁铁矿；拜耳法

(Edited by Wei-ping CHEN)